

Nanosized alumina from boehmite additions in alumina porcelain

Part 2: Effect on material properties

F. Belnou, D. Goeuriot^{*}, P. Goeuriot, F. Valdivieso

Ecole Nationale Supérieure des Mines de Saint-Etienne (Centre SMS, UMR 5146), 42023 Saint-Etienne Cedex 2, France

Received 26 January 2006; received in revised form 24 February 2006; accepted 28 March 2006

Available online 11 September 2006

Abstract

The influence of boehmite gel additions on the green and sintered properties of alumina porcelain is investigated. Green bodies are reinforced in the presence of gel through the building of hydrogen bonds within porcelain mixtures. The particular reactivity of this system leads to shrinkage inhibition and densification problems during sintering. Adjusting the formulation of these materials slightly modifies phase formation during thermal cycles but allows good densification because of extra glass production. Sintered samples have undergone thermomechanical tests: using boehmite gel additions increases both bending strength and thermal shock resistance of alumina porcelains by shifting the size of residual pores towards lower diameters and enhancing mullitisation.

© 2006 Elsevier Ltd and Techna Group S.r.l. All rights reserved.

Keywords: C. Mechanical Properties; D. Mullite; D. Porcelain; Reaction-sintering

1. Introduction

Alumina is often used in porcelain paste in order to enhance mechanical properties [1]. The aim of the present work is to study the influence of the replacement of a part of the classical alumina filler by a boehmite gel, in order to develop hydrogen bonds in green bodies and so enhancing their mechanical resistance. The influence of boehmite additions on the reaction-sintering of alumina porcelain was investigated in the first part of this paper [2]. Dilatometric curves of these boehmite alumina porcelains present a shrinkage inhibition that has been explained by the study of phase and porosity evolution from room temperature up to 1400 °C. It has been shown that when vitrification occurs the presence of alumina nanoparticles leads to extra mullitisation which has two major consequences: a volume expansion resulting in a shrinkage inhibition and a decrease of the amount of liquid which causes densification problems. This two-fold phenomenon is enhanced if the alumina filler is coarse but it is limited when fine and round alumina is used because in that case vitrification kinetics is slowed down.

This second part is devoted to the resolution of sintering problems by using new formulations containing wollastonite instead of chalk, in order to develop a sufficient amount of liquid phase during sintering. Sintering conditions of these new materials will be optimised. The elaboration and characterisation of boehmite alumina porcelains, green resistance and sintered thermomechanical properties—flexural strength and thermal shock resistance, will also be described.

2. Experimental procedures

The materials used in this study are industrial porcelain pastes (kaolin, potash and soda feldspars, chalk or wollastonite) with alumina additions (no quartz is added in the pastes): these additions are under the form of granular alumina (alumina filler) and/or boehmite gel. Two types of alumina filler are used: a fine one ($d_{50} = 0.48 \mu\text{m}$) and a coarse one ($d_{50} = 4\text{--}6 \mu\text{m}$).

Two sets of materials were used:

- mixtures used in the first part of this study: PC, PCG and PFG [2];
- new mixtures called PC(2), PCG(2) and PFG(2) (2 means “new”) that rely on the same formulation principles as PC, PCG and PFG but contain less boehmite gel. They are described in Table 1 (green densities are 1.84 ± 0.02). As

^{*} Corresponding author.

E-mail address: dgoeuriot@emse.fr (D. Goeuriot).

3. Results and discussion

3.1. Mechanical properties of green bodies

Table 2, showing the effect of gel additions on MOR values for green samples, puts in evidence the possibility of enhancing green mechanical properties via gel additions. MOR enhancement is obtained with both types of alumina filler, coarse and fine. Specific resistance is doubled by adding 10 wt% boehmite gel. The reason for the strengthening effect is shown by Infra-Red spectrometry analyses: in the presence of gel, the spectrum in Fig. 2a presents two extra peaks at 3300 and 3100 cm^{-1} , that are characteristic of hydrogen bonds. The gel is constituted with hydrated alumina AlOOH that can react with clay and feldspathic particles around to build a network of hydrogen bonds that is favourable to the cohesion of green bodies. Hydrogen bonds remain within the pastes even after drying process, as shown on Fig. 2b: this confirms their action on the strengthening of green samples.

3.2. Sintering conditions for new formulations PC2, PFG2 and PCG2

3.2.1. Sinterability of new formulations

The dilatometric behaviour of new materials is presented in Fig. 3. Behaviours of PC2 and PC (formulations containing respectively wollastonite or chalk) are similar. The maximum of shrinkage is obtained at the same temperature: in this case, as there is no boehmite gel, shrinkage slow down is due to primary mullitisation inside kaolin grains and so does not depend on other components. Differences observed on peaks intensities are linked to forming process: PC2 is pressed while PC is

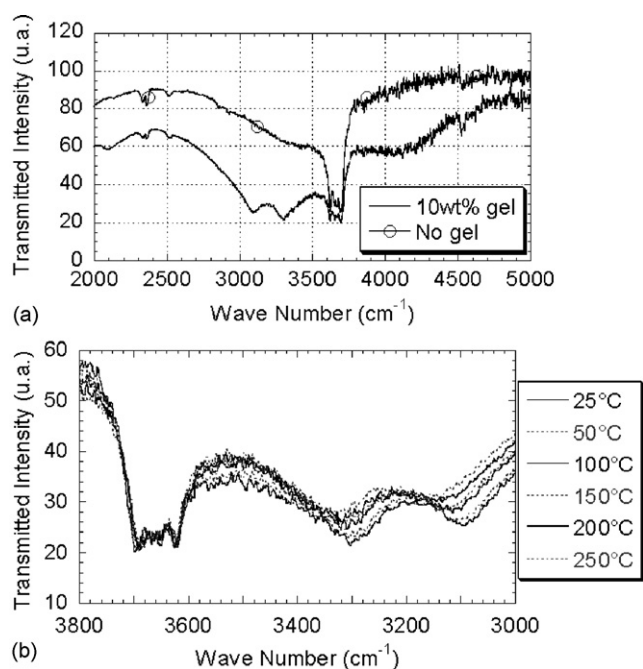


Fig. 2. IR spectroscopy of green bodies. (a) Comparison of IR spectra of gel free and gel containing green materials. (b) Evolution of IR peaks with temperature in gel containing green materials.

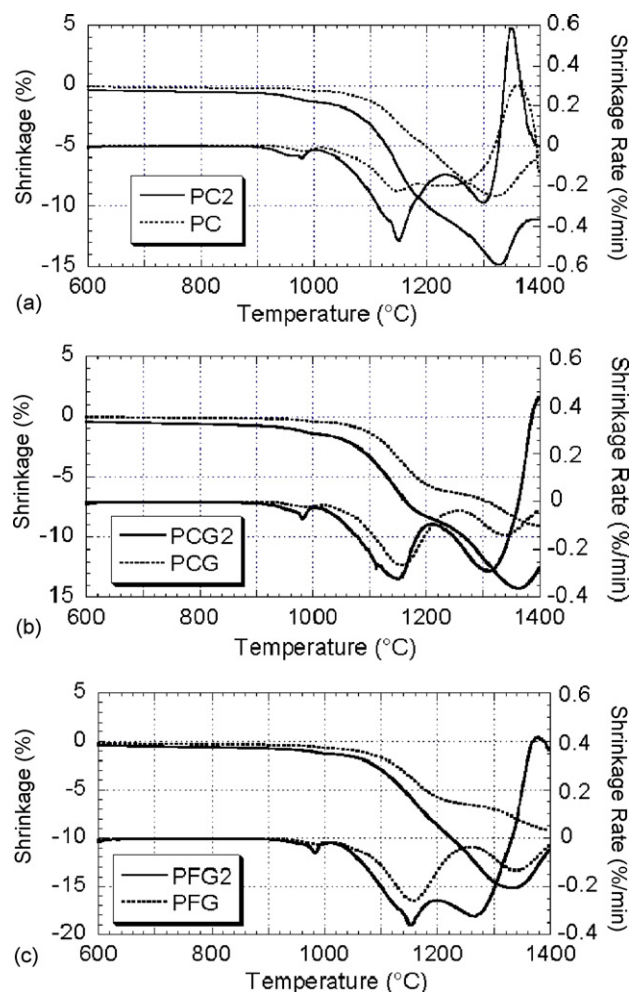


Fig. 3. Effect of new formulation on the dilatometric behaviour of porcelain pastes: comparison of: (a) PC and PC2, (b) PCG and PCG2 and (c) PFG and PFG2.

extruded; it was verified that these different processes have no influence on the temperature of peaks and thus on the associated phenomena. Comparing the behaviours of the other compositions highlights that the use of new formulations and the reduction of gel content make it possible to limit the amplitude of shrinkage slow down between 1150 and 1250 °C and to decrease the temperature at which shrinkage ends. This meets our expectation that the formulations containing wollastonite should sinter better than those containing chalk.

3.2.2. Choice of sintering conditions

To sinter materials for the evaluation of final thermomechanical properties, different cycles have been tried: the selected treatments are 30 min at 1300 °C for PC2, 1 h at 1300 °C for PCG2 and 1 h 30 at 1280 °C for PFG2. The selection criteria have been chosen within sight of optimising final thermomechanical properties that is, limiting the amount and size of pores.

3.3. Characterisation of sintered materials

3.3.1. Composition

Table 3 gives the phase compositions of the three materials PC2, PFG2 and PCG2: this case is difficult to compare with

Table 3
Characterisation of sintered bodies

	Siliceous porcelain	PC2	PCG2	PFG2
Phases contents after sintering (in wt%): error: $\pm 2\%$ for major phases and $\pm 1\%$ for minor phases		Alumina 35 Mullite 13 Quartz ~ 0 Anorthite 6 Glass 46	Alumina 30 Mullite 20 Quartz ~ 0 Anorthite 4 Glass 46	Alumina 35 Mullite 11 Quartz > 0 Anorthite 6 Glass 48
Porosity parameters				
Surfacic ratio of porosity (%)		15.5	18.9	9.2
No. of pores per $100 \mu\text{m}^2$		0.11	0.24	0.26
Mean diameter (μm)		11 ± 10	8.1 ± 8.2	5.7 ± 8.6
Flexural bending strength				
MOR (MPa)	45 ± 6	90 ± 23	106 ± 14	112 ± 19
Thermal shock resistance parameters				
ΔT_c ($^{\circ}\text{C}$)	210	240	270	240
R factor		141K	171K	146K
α	0.5	0.33	0.29	0.21

previous results on formulations with chalk PC, PCG and PFG, because thermal cycles are different; despite this, several remarks can be noted: The first difference with the previous formulations and their study without soaking time (see [2]) is the quasi disappearance of quartz in all cases here: at these temperatures quartz dissolution is possible [1,3] and the soaking time factor allows this dissolution whatever the quantity of liquid present in the system. The second difference is the amount of anorthite, slightly higher than before. This is due to the new formulations: liquid is enriched in CaO compared to the previous system (PC, PCG and PFG) because of the amount of wollastonite, and that leads to more anorthite. Moreover, this anorthite does not dissolve, which appears to be contradictory with the tendencies observed in part 1 of this study around 1300°C . In fact, the anorthite–orthose diagram [4] shows that the richer the composition is in anorthite the higher the temperature is needed to see that it dissolves and this is what occurs here. The third great difference with PC, PCG and PFG materials is the reduction in the quantities of mullite. It is due to two factors: a smaller amount of boehmite gel, 6% instead of 10%, and thus a least contribution of reacting alumina in the system; and the formation of a greater quantity of anorthite that competes with secondary and pseudotertiary mullite formation as both phases rely on the same mechanism to form (enrichment of liquid in alumina by dissolution). Another possible source of limitation of mullite content could be that soaking can allow partial dissolution of primary mullite to occur [3]. Consequently, to this least amount of mullite, glass content is higher within these new materials, especially for PCG2 compared to PCG.

3.3.2. Microstructures

The microstructures of sintered PC2, PCG2 and PFG2 are shown in Fig. 4. They are composed of the same microstructural features though with some differences especially concerning the progress of mullitisations. The matrix is of course glass that has been superficially dissolved by etching. EDS detects a mix

of mullite and alumina grains (the A + M zones on micrographs): this mullite is mainly primary mullite and alumina comes from the filler and probably also from some unreacted decomposition products of metakaolin. The original feldspar grains (still recognizable) have turned into aggregates of secondary mullite needles (the M zones): these needles have grown more or less – some bright and very small crystallites can be seen on PCG2 and PFG2 micrographs – depending on the type of material and thus on the progress of vitrification (for details on reactivity, see part 1 of this work [2]). Isolated and rare quartz grains can also be seen (the Q zones), sometimes with cracks inside and around them. Pseudotertiary mullite is difficult to identify as it is very small and mixed with primary mullite and alumina around the secondary mullite zones. These microstructural features are classical for alumina porcelains and meet with other authors reports [1,3,5].

3.3.3. Porosity

Porosity evolution during thermal cycles is shown in Fig. 5a and b. The evolution of total open porosity (Fig. 5a) in PCG2 is parallel to that in PCG until 1250°C , which means that the pore elimination kinetics is the same in these two materials that only slightly differ. However the beneficial effect of new formulations on sinterability clearly appears as the amount of porosity is much lower in PCG2 (starting from the same green density as PCG). Another evidence of this is that above 1250°C the pore elimination kinetics slows down in PCG2 which indicates that the end of sintering is close: this phenomenon could not be observed in PCG material. Fig. 5b also shows this beneficial effect: residual micropores which were difficult to eliminate in PCG are less above 1250°C with the new formulation PCG2 and their elimination kinetics increase throughout sintering.

Porosity in sintered samples is presented in Table 3 and Fig. 6: a comparison of PC2 and PCG2 shows that its amount is higher in the presence of gel. This means that the densification problem due to the presence of gel, though strongly limited by using new formulations with wollastonite, is in fact not fully

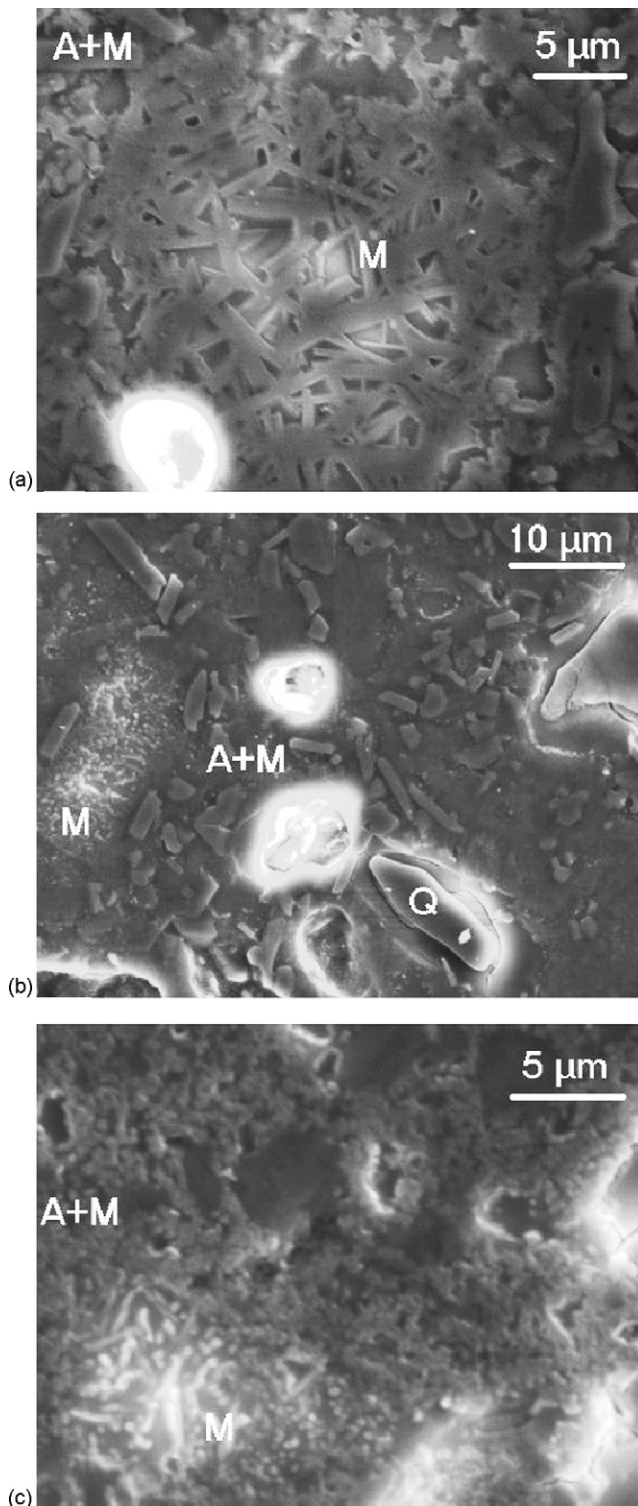


Fig. 4. Microstructures of sintered: (a) PC2, (b) PCG2 and (c) PFG2.

cured. The smallest amount of pores obtained for PFG2 is consistent with previous results on PFG composition [2] indicating that pore elimination kinetics increase above 1250 °C in this material. It is to be noted that the distribution of pores is concentrated a little on the smallest sizes when gel is used (PCG2 and PFG2), with respective d_{90} of 20 and 15 μm, instead of 25 μm for PC2.

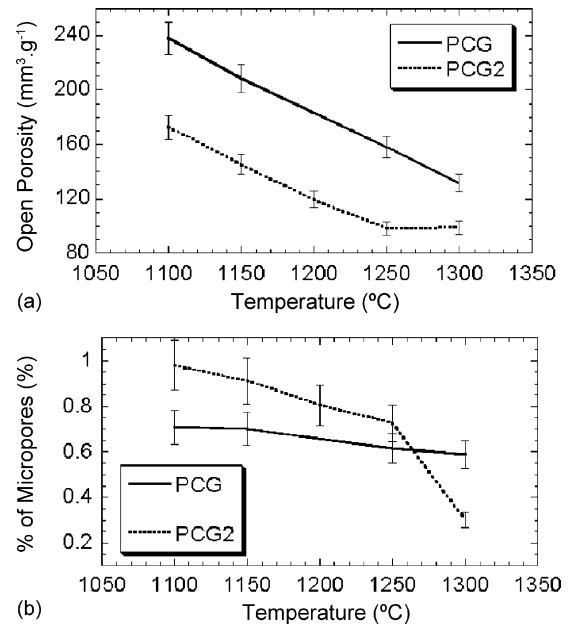


Fig. 5. Effect of new formulations on the evolution of porosity. (a) Evolution of total open porosity with temperature. (b) Evolution of microporosity ($\varnothing < 1 \mu\text{m}$) with temperature.

3.4. Thermomechanical properties

Two types of characterisation were carried out: a test of flexural strength and a test of resistance to damage by thermal shock, which appeared relevant within sight of the domestic application considered for porcelain materials [6,7].

Results of simple bending tests are given in Table 3: it has been added for comparison a reference porcelain without alumina which corresponds to industrial samples prepared from a paste containing quartz as degreasing agent. This addition makes it possible to remind and point out the well-known utility of alumina to increase the final bending strength of these materials: the modulus of rupture is doubled when replacing quartz by alumina (siliceous porcelain compared to PC2). Concerning the materials optimised in this study, PC2, PCG2 and PFG2, the results show an increase of 18% of performances in bending strength when adding boehmite gel.

Despite the material without gel (PC2) is a little less porous than that with gel (PCG2) it does not present a better resistance. But it should not be forgotten that the size of porosity plays an important part in the rupture process: as shown above pores contained in PCG2 are a little finer. Moreover, it could be considered that the mullite content, more important in PCG2, can also play a part in the strengthening effect. The difference observed between PCG2 and PFG2 can be directly connected with the porosity amount and size: the less porous material (PFG2) resists best, and porosity is also finer in PFG2.

The dispersion of results is the lowest for PCG2 and PFG2. The materials issued from pastes containing gel are thus perhaps also more homogeneous towards rupture criteria (size of the critical defect for instance, pores are finer when gel is used).

Sintered samples have also been tested in four-point bending after degradation through thermal shocks by water quenching.

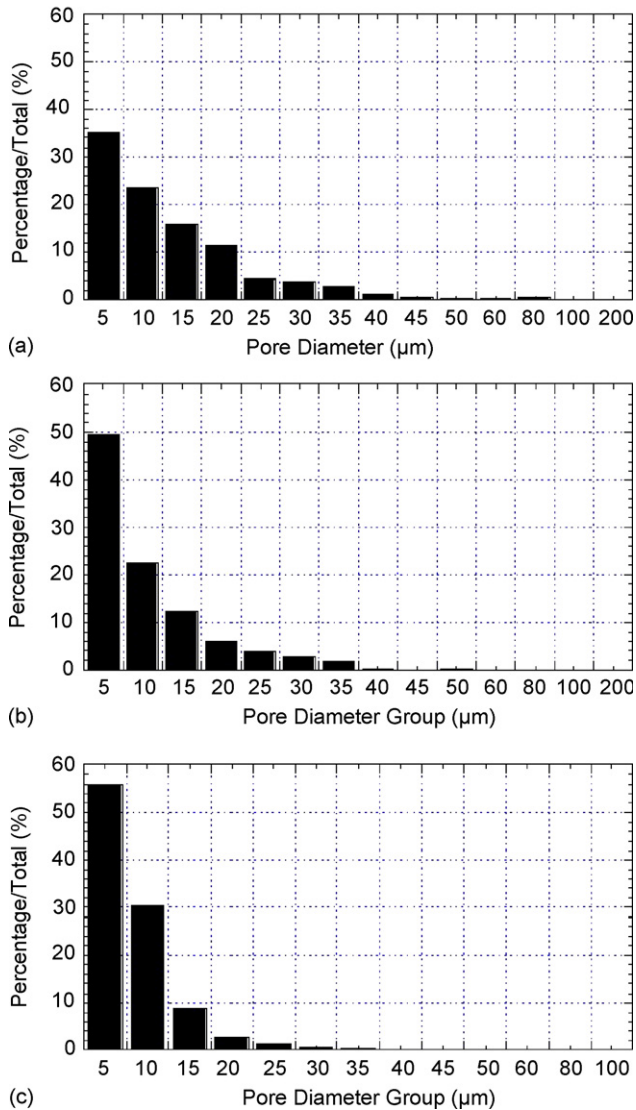


Fig. 6. Size distribution of pores in sintered: (a) PC2, (b) PCG2 and (c) PFG2.

Obtained curves are presented on Fig. 7. The two typical parameters for thermal shock resistance, ΔT_C and α , are given for each material in Table 3, and the R parameter [8] was calculated as follows:

$$R = \frac{\sigma_f(1 - \nu)}{E\alpha}$$

where σ_f is the rupture modulus; ν the Poisson coefficient, considered constant for the three materials PC2, PFG2 and PCG2 and E is the Young's modulus, that can be calculated as a function of porosity following the RICE model [9]:

$$E = E_0 \exp(-3P)$$

with E_0 is the Young's modulus for fully dense materials, considered as constant for the three materials; it is not known here and P is the porosity amount. for the three materials, it gives:

$$\text{PC2: } E = E_0 \exp(-0.45) = 0.638E_0;$$

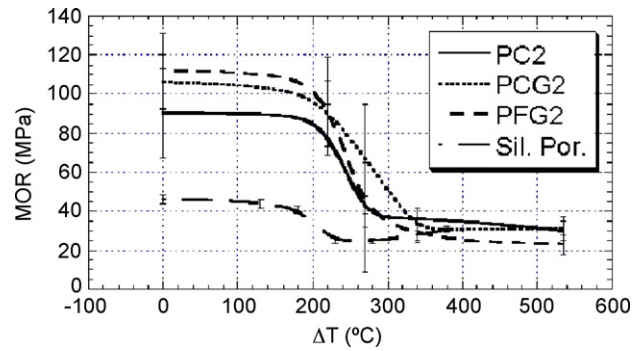


Fig. 7. Thermal shock resistance of sintered materials.

$$\text{PCG2: } E = E_0 \exp(-0.48) = 0.619E_0;$$

$$\text{PFG2: } E = E_0 \exp(-0.27) = 0.763E_0;$$

α is the linear dilatation coefficient, considered as constant for the three materials

The calculation of R for each case gives (taking into account that some properties are unknown):

$$\text{PC2} = 90/0.638K = 141K \text{ with } K = (1 - \nu)/E_0\alpha;$$

$$\text{PCG2} = 106/0.619K = 171K;$$

$$\text{PFG2} = 112/0.763K = 146K.$$

The different calculated R values are almost in agreement with the evolution of the critical temperature difference ΔT_C (for example: increase of ΔT_C of 12.5% from PC2 to PCG2, while R increase is 21%) and permit to point out that PCG2 present the best resistance because of both its porosity amount and the effect on MOR due to the reactivity induced by the initial gel. The mechanical degradation after thermal shock at higher temperature than ΔT_C is the lowest for the material issued from pastes containing gel. But the final resistance is the same in the three cases: about 40 MPa.

4. Conclusions

Boehmite gel additions to classical alumina porcelain allow mechanical reinforcement of green bodies, a critical parameter in many ceramic processes. This strengthening is due to hydrogen bonds established between boehmite and clay and/or feldspathic particles within the green material and remaining after drying process.

Although as demonstrated elsewhere these gel additions lead to sintering problems, it is possible to avoid this difficulty with slight and simple changes in porcelainic formulations: adjustment of the gel content and kaolinite/feldspar ratio and using wollastonite instead of chalk enhances vitrification and thus densification during reaction-sintering. Phase formation processes are very little affected by these changes: anorthite amount increases a little as mullitisation is more limited mainly because of the higher CaO and lower boehmite amounts in the system and also because there is a competition between anorthisation and secondary and tertiary mullitisations that leads to preferential formation of anorthite by alumina dissolution in glass.

Boehmite alumina porcelain can be fired around 1300 °C and sintered bodies present interesting thermomechanical properties: boehmite gel additions have a beneficial effect on both bending strength and thermal shock resistance which comes in addition to the well-known reinforcement effect of alumina granular filler in traditional porcelains.

Acknowledgments

The authors would like to thank Groupe Cerama and Région Rhône-Alpes for financial support of this study.

References

- [1] W.M. Carty, U. Senapati, Porcelain—raw materials, processing, phase evolution and mechanical behavior, *J. Am. Ceram. Soc.* 81 (1) (1998) 3–20.
- [2] F. Belnou, D. Goeuriot, P. Goeuriot, F. Valdivieso, Nanosized alumina from boehmite additions in alumina porcelain – 1. Effect on reactivity and mullitisation, *Ceram. Int.* 30 (2004) 883–892.
- [3] Y. Iqbal, W.E. Lee, Microstructural evolution of triaxial porcelain, *J. Am. Ceram. Soc.* 83 (12) (2000) 3121–3127.
- [4] E.M. Levin, C.R. Robbins, H.F. McMurdie, Phase Diagrams for Ceramists, first ed, The American Ceramic Society Inc., 1964 Fig. 799.
- [5] Y. Iqbal, W.E. Lee, Fired porcelain microstructures revisited, *J. Am. Ceram. Soc.* 82 (12) (1999) 3584–3590.
- [6] Y. Kobayashi, M. Yamada, M. Nakayama, et al., Strength and thermal shock resistance of alumina strengthened porcelain containing cristobalite, *J. Ceram. Soc. Jpn.* 111 (12) (2003) 872–877.
- [7] H. Baharav, B.Z. Laufer, A. Mizrahi, H.S. Cardash, Effect of different cooling rates on fracture toughness and microhardness of glazed alumina reinforced porcelain, *J. Prosthet. Dent.* 76 (1) (1996) 19–22.
- [8] D.P.H. Hasselman, Thermal shock resistance parameters for brittle refractory ceramics: a compendium, *Am. Ceram. Soc. Bull.* 49 (12) (1970) 1033–1037.
- [9] R.W. Rice, Grain size and porosity dependence of ceramic fracture energy and toughness at 22 °C, *J. Mater. Sci.* 31 (1996) 1969–1983.